

All-electron density-functional studies of hydrostatic compression of pentaerythritol tetranitrate $C(CH_2ONO_2)_4$

Chee Kwan Gan,^{*} Thomas D. Sewell,[†] and Matt Challacombe[‡]*Theoretical Division, Los Alamos National Laboratory, Los Alamos, New Mexico 87545, USA*

(Received 1 August 2003; revised manuscript received 29 October 2003; published 30 January 2004)

All-electron calculations of the hydrostatic compression of pentaerythritol tetranitrate $C(CH_2ONO_2)_4$ (PETN) crystal have been performed using density-functional theory with the PBE functional in conjunction with the 6-31G** Gaussian basis set. Full optimizations of the atomic positions and ratio of lattice parameters c/a for the tetragonal crystal were performed for eight volume ratios $0.65 \leq V/V_0 \leq 1.00$, where V_0 is the equilibrium volume at zero pressure. The pressure, linear compressibilities of lattice parameters a and c , and c/a ratio as functions of volume ratio are in good agreement with experiment. It is observed that c/a decreases monotonically with compression until $V/V_0 = 0.8$, and then increases monotonically for all higher levels of compression considered. Changes in intramolecular coordinates and close intermolecular contact distances were studied as a function of compression. The results indicate essentially rigid-molecule compression for $V/V_0 > 0.8$, with the onset of significant intramolecular distortion for higher compressions. Predictions of the bulk modulus B_0 and its pressure derivative B'_0 were obtained using various equation of state fitting forms. Values for these quantities are compared to experiment and to the results of a preceding molecular simulation study of PETN based on an empirical force field.

DOI: 10.1103/PhysRevB.69.035116

PACS number(s): 71.15.Nc, 31.15.Ew

I. INTRODUCTION

Pentaerythritol tetranitrate [PETN, $C(CH_2ONO_2)_4$] is an important secondary high explosive. At room temperature, PETN crystallizes in a tetragonal space group $P\bar{4}2_1c$, with two molecules per unit cell.¹⁻³ A high-temperature form denoted PETN-II has also been reported.⁴ PETN has received a lot of attention due to interesting anisotropic, nonmonotonic shock initiation sensitivity.⁵⁻¹⁰ The room-temperature linear and volumetric hydrostatic compression of PETN has been measured by Olinger and co-workers^{11,12} using x-ray diffraction for pressures up to 10.45 GPa. Dick and von Dreele¹³ used neutron scattering from deuterated PETN to study detailed pressure-induced changes in dihedral angles and molecular orientations in the unit cell for pressures up to 4.28 GPa. While the volumetric compression reported by Dick and von Dreele is consistent with the data of Olinger *et al.*, significant differences are observed in the linear compressions along the a and c crystal axes.

A complete set of isentropic elastic coefficients for PETN has been reported by Morris¹⁴ based on extensive single crystal sound speed measurements. The resulting elastic tensor was of high precision with the exception of element C_{13} , which had an uncertainty over ten times the average for the others. Winey and Gupta¹⁵ reanalyzed Morris' data, identified the source of the inconsistency in C_{13} , and reported an internally consistent and precise elastic tensor.

There have been a number of theoretical studies of PETN crystals based on empirical force fields. Dick and Ritchie¹⁶ performed molecular mechanics calculations using the AMBER4.0 force field to study the energetics associated with slip along specific directions in the crystal, in an effort to understand the anisotropic initiation sensitivity in PETN. Their results were largely consistent with experimental data, but were not conclusive due to the lack of rate-dependent information.

Theoretical predictions of PETN crystal structure, thermal expansion, and hydrostatic compression were reported by Sorescu *et al.*^{17,18} They used an intermolecular potential function developed in their laboratory in conjunction with a rigid-molecule approximation for the molecular structure. Agreement to within one percent of experiment was obtained for the crystal lattice parameters at 298 K, although the calculated thermal expansion coefficient was three times smaller than the experimental value. Sorescu *et al.*¹⁸ predicted linear compressibilities that were in reasonable agreement with experiment for pressures below 6 GPa, with the onset of significant discrepancies for higher pressures. (The calculated linear compressibilities were systematically lower than the measured ones, resulting in a larger error in the volumetric compressibility over the entire pressure interval, and leading to a 41% error compared to experiment in the predicted initial bulk modulus.) The authors attributed the errors in their predictions at higher pressure to a shortcoming of the rigid-molecule approximation.

Bunte and Sun¹⁹ reported a flexible molecule inter- and intramolecular COMPASS force field parametrization based on a calibration to experimental data and high level gas phase electronic structure results for selected nitrate esters. Although PETN was not part of the force field training set, predicted crystal lattice parameters for PETN were in good agreement with experiment. Bunte and Sun reported five of the six elastic coefficients for PETN at zero K, based on energy-minimized lattice parameters as well as for a constrained calculation in which the lattice parameters were set equal to experimental values. Reasonable agreement with experimental data was obtained in the latter case, in spite of neglect of explicit thermal effects. Since they did not report the C_{13} elastic coefficient, it is not possible to obtain a bulk modulus from their work.

Zaoui and Sekkal²⁰ reported calculations of PETN thermal and mechanical properties using a flexible molecule,

Tersoff-like force field. This work is difficult to interpret, as the primary simulation cell described in the article corresponds to a nonintegral number of molecules, and the predicted longitudinal and transverse sound speeds are both unrealistically small and inconsistent with the reported bulk modulus. For these reasons, it will not be considered further below.

Kuklja and Kunz²¹ studied the electronic structure of PETN crystal containing an edge dislocation using Hartree-Fock theory with CRYSTAL95/98.²² They considered edge-type dislocations with Burgers vector [001], and found that a shear stress, induced by the dislocations, produces local electronic states in the fundamental band gap of the crystal.

In this contribution, we report condensed phase electronic-structure calculations of the hydrostatic compression of PETN at absolute zero and pressures up to 25 GPa. We employ an all-electron density-functional method using the PBE functional (Ref. 23) in conjunction with the 6-31G** Gaussian basis set. Complete optimization of the cell contents and c/a ratio of the lattice parameters is performed at each of the eight volumes considered, assuming a tetragonal cell (i.e., $a=b \neq c$, $\alpha=\beta=\gamma=90^\circ$). It should be noted that our all-electron treatment is computationally more demanding than pseudopotential methods, but it should be free from potential errors associated with pseudopotentials that may become important at high pressures.

The remainder of this paper is organized as follows. In Sec. II we describe the computational framework and in Sec. III the details of our calculations. In Sec. IV we present the results of the calculations and properties derived from them, with comparisons to experiment and previous theoretical studies. Finally, in Sec. V we summarize the main conclusions of our work.

II. COMPUTATIONAL FRAMEWORK

Calculations were performed using a parallelized version of MONDOSCF,²⁴ a suite of programs for linear scaling electronic-structure theory and *ab initio* molecular dynamics. Periodic boundary conditions²⁵ were used to study the PETN crystal. The MONDOSCF code employs a number of advanced $\mathcal{O}(N)$ techniques such as the quantum chemistry tree code (QCTC) for the Coulomb matrix build²⁶⁻²⁸ and the adaptive Hierarchical Cubature (HiCu) for the exchange-correlation matrix build.²⁹ Parallelization of MONDOSCF has been carried out, where an exemplary success is the efficient data-parallel algorithm for the HiCu method³⁰ with an equal-time partitioning scheme that exploits the temporal locality of SCF calculations to achieve excellent load balance. We used a cluster of 256 4-CPU HP/Compaq Alphaserver ES45s with the Quadrics QsNet High Speed Interconnect to perform the calculations in this work. Most calculations were performed using 32 processors.

III. COMPUTATIONAL PROTOCOL

The results described below are for three-dimensionally periodic, gradient-corrected density-functional theory (GGA), using the PBE functional.²³ The small 3-21G split-

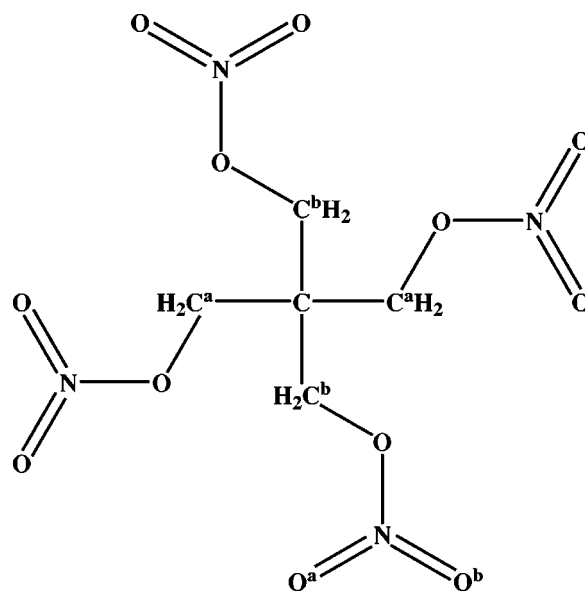


FIG. 1. Chemical structure of PETN. Superscripts “a” and “b” are used in Table II to distinguish geometrically distinct internal coordinates for comparison to experiment.

valence Gaussian basis set was tried first, but found to be inadequate relative to the larger 6-31G** basis set. Thus, the 6-31G** basis set was used for all results reported here. The Γ point for Brillouin zone sampling was used throughout with the crystallographic unit cell, which contains two molecules (58 atoms). However, a number of calculations were carried out using a $1 \times 1 \times 2$ supercell to verify convergence of the Γ -point approximation [as shown in Fig. 2(a)]. Because of the necessity to resolve millihartree energy differences, a “good” level of numerical approximation was used throughout to achieve the required 7-8 digits of accuracy in the total energy, which was approximately -2600 Ha. This combination of large basis set and accurate numerical approximation was mastered through parallel $\mathcal{O}(N)$ algorithms, a key enabling technology for these types of calculations.

Starting with the experimental x-ray crystal structure reported by Conant *et al.*,³ we calculated the zero pressure unit cell volume V_0 under the assumption of a tetragonal lattice ($a=b \neq c$, $\alpha=\beta=\gamma=90^\circ$) by computing fully energy-minimized structures on a 5×5 grid of a and c lattice parameters, and fitting the results to a cubic polynomial in a and c . A subsequent calculation on a 3×3 grid centered at the minimum predicted from the preceding step was used to obtain an improved prediction of the optimized crystal structure. These correspond to a_0 , c_0 and $V_0 = a_0^2 c_0$. Stability of the tetragonal structure was checked by energy minimization of nearby orthorhombic structures ($a \neq b \neq c$) in the vicinity of the tetragonal minimum; these tests confirmed that the tetragonal structure is favored energetically over neighboring orthorhombic ones.

Energy-minimized structures for a given volume ratio V/V_0 were obtained by scanning a set of c/a ratios consistent with the desired volume V . Initial guesses were obtained by rigid translation of the molecular structure obtained from the next larger volume ratio via a transformation that pre-

TABLE I. Equilibrium lattice parameters and unit cell volumes for PETN.

$a(\text{\AA})$	$c(\text{\AA})$	$V(\text{\AA}^3)$	Source	Comment
9.425	6.758	600.3	This work	PBE/6-31G**
9.383	6.711	590.8	Olinger <i>et al.</i> (Ref. 11)	X-ray diffraction, $\sim 298\text{K}$
9.3776	6.7075	589.9	Conant <i>et al.</i> (Ref. 3)	X-ray diffraction, $\sim 298\text{K}^a$
9.3348	6.6500	579.47	Sorescu <i>et al.</i> (Ref. 18)	NPT-MD, 298K, rigid molecules
9.35	6.67	583	Bunte and Sun (Ref. 19)	NPT-MD, 293K

^aRoom-temperature measurement; precise temperature unspecified.

serves the center-of-mass positions in crystallographic coordinates. Typically, seven values of c/a were considered at a given volume, and the results were fit to a parabola.

IV. RESULTS

Calculated and measured lattice parameters are compared in Table I, where we also include the experimental results of Olinger *et al.*¹¹ and Conant *et al.*,³ and the theoretical predictions of Sorescu *et al.*¹⁸ and Bunte and Sun¹⁹ for completeness. Percent errors in our calculations relative to the experimental results of Conant *et al.*³ are 0.51, 0.75, and 1.8% for a_0 , c_0 , and V_0 , respectively. It is important to note, however, that we have not attempted to correct for thermal expansion, since experimental coefficients of thermal expansion for PETN do not extend to cryogenic temperatures.

Calculated intramolecular coordinates and selected intermolecular distances are compared to the experimental results of Conant *et al.*³ in Table II (see also Fig. 1). The predicted molecular geometry is in excellent agreement with experiment. The 12% discrepancy in the C—H distances is expected, since we are comparing to x-ray data. Otherwise, most of the intramolecular degrees of freedom are accurately predicted to within a few percent. There are three intermo-

lecular distances less than 3\AA at equilibrium, each of which is an $\text{O}\cdots\text{H}$ contact. Predicted values are 2.396, 2.779, and 2.898\AA , with errors relative to experiment of -3.5 , -0.7 , and 0.1% , respectively.

The volumetric hydrostatic compression is summarized in Fig. 2. The variation of the energy with volume ratio is shown in Fig. 2(a). The line is a sixth degree polynomial fit, from which the pressure shown in Fig. 2(b) is obtained as $P = -dE/dV$. The open circles in Fig. 2(b) are the experimental data of Olinger *et al.*,¹¹ with experimental uncertainties comparable to the symbol sizes. The calculated volumetric compression is in remarkably good agreement with experiment. The effects of temperature would be expected to “soften” the calculated isotherm at low pressures; however, this effect should diminish quickly with increasing compression. While perhaps obvious, it is worth pointing out that this behavior has been observed for similar systems, including β -octahydro-1,3,5,7-tetranitro-1,3,5,7-tetrazocine (β -HMX).^{31,32}

The linear compression along the a and c crystallographic directions is shown in Fig. 3. Figure 3(a) reveals good agreement between our predictions and the experimental data for the relative compressions of a/a_0 and c/c_0 . In Fig. 3(b) we

TABLE II. Comparison between experiment and PBE/6-31G** MONDOSCF calculation of selected intramolecular and intermolecular parameters for PETN crystal (refer to Fig. 1). Units are \AA and degrees. Numbers in parentheses are percent errors relative to experiment.

Source	C—C	C—H	C—O	O—N	N=O
This work	1.532 (0.1)	1.098 (12.0)	1.444 (0.1)	1.437 (2.4)	1.219 (1.9)
Expt. (Ref. 3)	1.531	0.98	1.446	1.403	1.196
Source	CCH	HCH	CCO	HCO	
This work	111.0 (-1.1)	108.1 (1.5)	106.6 (-0.1)	110.1 (0.5)	
Expt. (Ref. 3)	112.2	106.5	106.7	109.6	
Source	CON	ONO ^a	ONO ^b	ONO	
This work	111.8 (-1.2)	117.4 (-0.3)	111.9 (-0.1)	130.7 (0.3)	
Expt. (Ref. 3)	113.2	117.7	112.0	130.0	
Source	C ^a CC ^a	C ^a CC ^b	CCON	CONO ^a	CONO ^b
This work	108.1 (0.4)	112.2 (-0.4)	169.9 (0.3)	3.4 (0.0)	176.6 (-0.1)
Expt. (Ref. 3)	107.7	112.7	169.4	3.4	176.8
Source	O \cdots H	O \cdots H	O \cdots H		
This work	2.396 (-3.5)	2.779 (-0.7)	2.898 (0.1)		
Expt. (Ref. 3)	2.482	2.798	2.894		

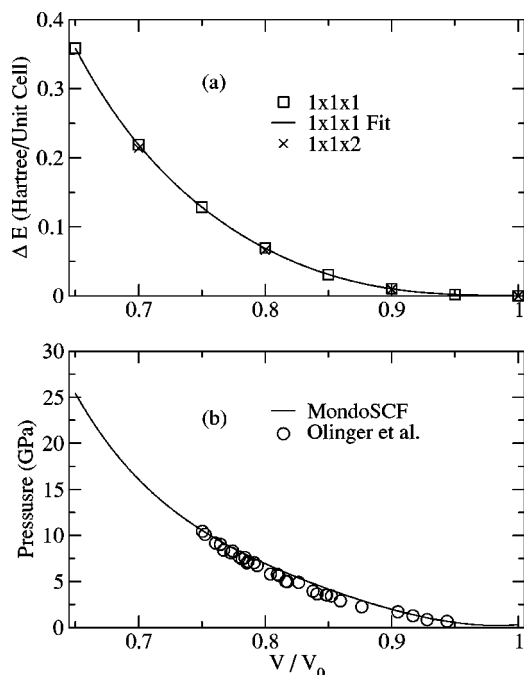


FIG. 2. Volumetric hydrostatic compression for PETN. (a) Energy difference ΔE . The solid line is a sixth degree polynomial fit to the $1 \times 1 \times 1$ predictions. Crosses are calculations for a $1 \times 1 \times 2$ supercell, and indicate that finite-size effects are minimal. (b) Pressure-volume relationship calculated from the fit in (a). Uncertainties in the experimental data of Olinger *et al.* (Ref. 11) are comparable to the symbol sizes.

show the variation of the c/a ratio as a function of compression. The solid line is based on polynomial representations of $a = a(V)$ and $c = c(V)$ due to Olinger *et al.*¹¹ We observe in both cases an initial decrease in the c/a ratio with increasing compression, followed by an increase toward a more “cubic-like” lattice structure. The positions of the minima in the curves are in fairly good agreement, and correspond to a volume ratio of 0.8 and a pressure of about 7 GPa.

In Figs. 4(a) and 4(b), we show the changes in intramolecular bond lengths and three-center angles as PETN is compressed. For clarity of presentation, we only include coordinates that undergo significant changes. It is observed that the bond lengths and angles remain almost constant for $0.8 \leq V/V_0 \leq 1.0$, with the onset of sizable changes for higher compressions. Backbone dihedral angles (not shown) exhibit qualitatively similar behavior, with changes of $2^\circ - 5^\circ$ beginning at $V/V_0 = 0.8$. (We note that Dick and von Dreele¹³ observed nonmonotonic variations of up to several degrees in some of the dihedral angles in deuterated PETN between zero and 4.28 GPa. We do not see any evidence for this in our calculations, based on the four compressions in our study that correspond to this pressure interval.) Figure 4(c) depicts the pressure response of the three sets of intermolecular van der Waals contacts that are below 3 \AA at zero pressure; each of these corresponds to an $\text{O} \cdots \text{H}$ interaction. The two longer distances decrease essentially linearly over the entire interval of compression studied, whereas the shorter one exhibits an obvious change in slope at about $V/V_0 = 0.8$, which

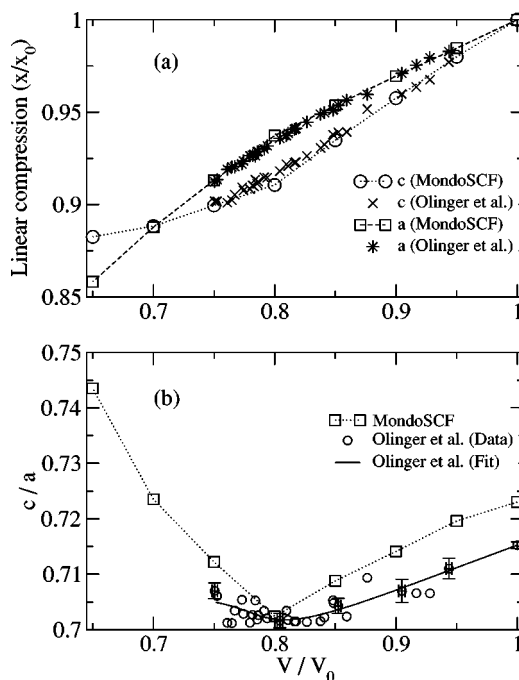


FIG. 3. Linear compression of PETN. (a) Relative linear compression of the lattice parameters. Squares and circles correspond to the a and c crystallographic axes, respectively; dashed lines are simply a guide for the eye. Experimental data from Olinger *et al.* (Ref. 11); experimental uncertainties are comparable to the size of the symbols. (b) Ratio of c to a . Squares denote calculated results; dashed line is a guide for the eye. Circles are experimental data (Ref. 11); error bars in c/a and V/V_0 are representative; solid line is a polynomial form taken from Ref. 11.

we again note is the volume ratio corresponding to the minimum in c/a .

The results in Fig. 4 are consistent with the discussion of Pastine and Bernecker,³³ who argued that the initial compression of an organic explosive is due almost entirely to reduction of intermolecular distances. At higher pressures, the energetic cost of further reduction of intermolecular distances becomes comparable to that associated with distortions of intramolecular degrees of freedom. From our calculations, we conclude that this transition occurs at approximately 7 GPa [see Fig. 2(b)]. Interestingly, Sorescu *et al.*¹⁸ observed that the deviations under hydrostatic compression of their simulated lattice parameters from the experimental values increased rapidly for pressures above 6 GPa. They attributed this to a shortcoming of the rigid-molecule approximation used in their work, and the present results corroborate this conclusion. Intuitively, one might expect a range of pressures over which different kinds of intramolecular degrees of freedom become involved, with dihedral, three-center angle, and covalent bond distortions emerging at successively higher pressures. That this is evidently not the case for PETN may be a consequence of the high symmetry of the crystal.

We can obtain the bulk modulus $B_0 = -VdP/dV$ and its initial pressure derivative $B'_0 = dB_0/dP$ from the PV data using equation of state fitting forms. In order to connect with preceding work, we consider three forms. The first form is the Murnaghan equation³⁴

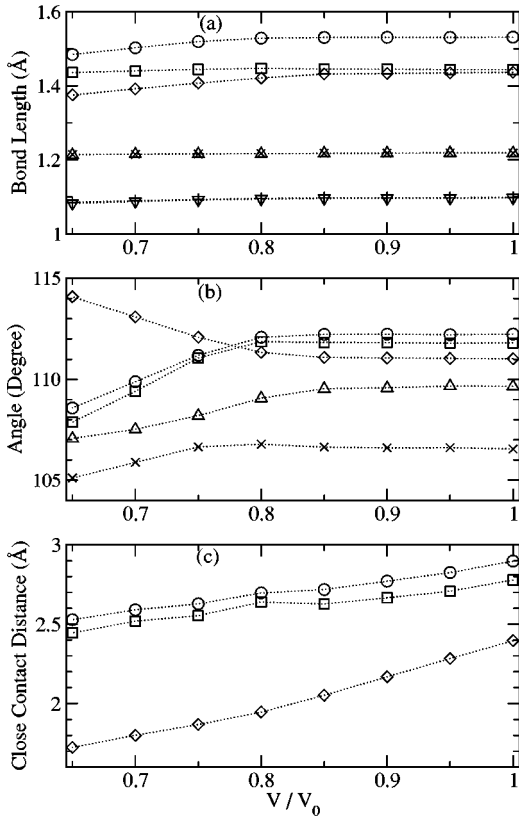


FIG. 4. (a) Variation of bond lengths in PETN as a function of hydrostatic compression. Circle: C-C; square: C-O; diamond: O-N; up-triangle and cross: N=O; down-triangle and plus: C-H. (b) Variation of three-center angles. Circle: C-C-C; square: C-O-N; diamond: C-C-H; up-triangle: H-C-O; cross: C-C-O. (c) Compression of intermolecular van der Waals contacts whose value is less than 3 Å at zero pressure. All three correspond to O...H contacts.

$$P = \frac{B_0}{B'_0} (\eta^{-B'_0} - 1), \quad (1)$$

where $\eta = V/V_0$. The second form is the third-order Birch-Murnaghan equation³⁵ used previously in the analysis of the isotherm for the high explosive octahydro-1,3,5,7-tetranitro-1,3,5,7-tetrazocine (HMX)^{36–38}

$$P = \frac{3}{2} B_0 (\eta^{-7/3} - \eta^{-5/3}) \left[1 + \frac{3}{4} (B'_0 - 4) (\eta^{-2/3} - 1) \right]. \quad (2)$$

The third fitting form

$$P = \frac{(V_0 - V)c^2}{[V_0 - s(V_0 - V)]^2} \quad (3)$$

is derived from the shock Hugoniot conservation equations

$$U_s = \sqrt{PV_0/(1 - V/V_0)} \quad (4)$$

and

$$U_p = \sqrt{PV_0(1 - V/V_0)}, \quad (5)$$

where U_s and U_p are pseudo-shock and pseudo-particle velocities, respectively. The latter were used by Olinger *et al.* in the analysis of their isotherm data for PETN (Refs. 11,12) and other explosives including TATB,¹² β -HMX and RDX,³⁹ and nitromethane.⁴⁰ Equation (3) is a straightforward recasting of Eqs. (4)–(5) into the PV plane, assuming that $U_s = c + sU_p$. For this equation of state, the initial bulk modulus and its pressure derivative are given by $B_0 = c^2/V_0$ and $B'_0 = 4s - 1$, respectively.

Fits to isotherm data are sensitive to the fitting form chosen and the interval of data used in the fit, particularly if the interest is in obtaining precise predictions of the initial bulk modulus and its pressure derivative. To maintain consistency with the experiments of Olinger *et al.*,¹¹ we restrict our fits in the following to pressures below 10.45 GPa. Also, in addition to performing equation-of-state fits to our calculated isotherm, we applied Eqs. (1)–(3) to the experimental data of Olinger *et al.*

Calculated and measured values for the initial bulk modulus and its pressure derivative for PETN are summarized in Table III. The results of fits in the PV plane using Eqs. (1)–(3) to our calculated isotherm are fairly consistent, with $B_0 = 14.5$ – 16.0 GPa and $B'_0 = 5.2$ – 6.7 . Applying the same fitting forms to the experimental data of Olinger *et al.*,¹¹ we obtain $B_0 = 9.4$ – 12.2 GPa and $B'_0 = 6.4$ – 11.3 . Sorescu *et al.*¹⁸ reported $B_0 = 14.1$ GPa and $B'_0 = 10.4$ for a fit of their rigid-molecule simulation results to the Murnaghan equation of state [Eq. (1)]. Values of $B_0 = 8.8$ GPa and $B'_0 = 9.9$ can be

TABLE III. Calculated and measured bulk moduli B_0 and pressure derivative B'_0 for PETN.

B_0 (GPa)	B'_0	Data source	Fitting form	Comment
15.8	5.3	This work	Eq. (1)	Fit to PBE/6-31G** results for $P \leq 10.45$ GPa
14.5	6.7	This work	Eq. (2)	Fit to PBE/6-31G** results for $P \leq 10.45$ GPa
16.0	5.2	This work	Eq. (3)	Fit to PBE/6-31G** results for $P \leq 10.45$ GPa
11.7	6.8	Olinger <i>et al.</i> (Ref. 11)	Eq. (1)	Fit to experimental isotherm
9.4	11.3	Olinger <i>et al.</i> (Ref. 11)	Eq. (2)	Fit to experimental isotherm
12.2	6.4	Olinger <i>et al.</i> (Ref. 11)	Eq. (3)	Fit to experimental isotherm
8.8	9.9	Olinger and Cady (Ref. 12)		Deduced from Ref. 12, Table II and Eq. (18)
9.1		Winey and Gupta (Ref. 15)		Calculated from isentropic value
14.1	10.4	Sorescu <i>et al.</i> (Ref. 18)	Eq. (1)	Taken from Ref. 18, NPT-MD at 298K

deduced from the results presented by Olinger and Cady¹² based on the experimental isotherm. Note that the latter are revised values of B_0 and B'_0 , and are different from the ones initially published in Ref. 11 and subsequently used for comparison by Sorescu *et al.* in Ref. 18.

Another experimental value for B_0 can be obtained from the isentropic elastic tensor reported by Winey and Gupta,^{14,15} specifically,

$$B_0 = \frac{C_{33}(C_{11} + C_{12}) - 2C_{13}^2}{C_{11} + C_{12} + 2C_{33} - 4C_{13}}. \quad (6)$$

This yields an isentropic bulk modulus $B_0^s = 9.8$ GPa, which can be transformed to an isothermal bulk modulus B_0^i using the relation $B_0^i/B_0^s = C_V/C_P$, where C_V and C_P are specific heats at constant volume and constant pressure, respectively. Using values for C_V and C_P recommended in Ref. 12 gives the result $B_0^i = 9.1$ GPa, which we regard as the most accurate value for the zero pressure isothermal bulk modulus of PETN at room temperature.

It is unsurprising that the values of B_0 estimated from the zero Kelvin isotherm are larger than the values obtained from room-temperature data. Likewise, the fact that the value of B_0 reported by Sorescu *et al.*¹⁸ is larger than experiment even though it is based on a simulated room-temperature isotherm can be tentatively attributed to the use of a rigid molecule simulation protocol.

V. CONCLUSIONS

Hydrostatic compression of pentaerythritol tetranitrate (PETN) crystal has been studied using all-electron density-functional theory with the PBE functional and 6-31G** basis set. Even though our all-electron studies are computationally more demanding than a pseudopotential approach, they are free from associated errors that may arise at high compression. Optimized molecular geometries and tetragonal lattice

parameters were obtained at eight levels of compression corresponding to pressures between zero and 25 GPa. Predictions of the lattice parameters and pressure as a function of volume ratio V/V_0 are in good agreement with experiment. The results indicate essentially rigid-molecule compression below 7 GPa (or for $V/V_0 > 0.80$), with the onset of significant intramolecular distortions for higher pressures. Interestingly, this transition correlates with the position of a minimum, observed experimentally and in the present study, in the ratio c/a of the lattice parameters.

Values of the initial bulk modulus and its pressure derivative obtained by application of three different equation of state fitting forms to the calculated zero Kelvin isotherm are in reasonably good agreement with values obtained by application of those same fitting forms to the experimental data. In both cases, the choice of fitting form can change the predicted bulk modulus by ~ 10 –25%. The average theoretical bulk modulus, which corresponds to zero K, is 32% larger than the corresponding average experimental value based on the room-temperature isotherm. The success of these all-electron calculations for PETN demonstrates the precision of our $\mathcal{O}(N)$ algorithms, and suggests that it may be practical to undertake similar calculations on significantly larger, more complicated systems that are well outside the capabilities of conventional algorithms.

ACKNOWLEDGMENTS

This work has been carried out under the auspices of the U.S. Department of Energy under Contract No. W-7405-ENG-36 and the ASCI project. Most work was performed on the computing resources at the Advanced Computing Laboratory of Los Alamos National Laboratory, Los Alamos, NM 87545. We thank Alejandro H. Strachan for many fruitful discussions and Jerry Dick for useful comments on the manuscript.

*Electronic address: CKGan@LANL.gov

†Electronic address: Sewell@LANL.gov

‡Electronic address: MChalla@LANL.gov

¹A. D. Booth and F. J. Llewellyn, *J. Chem. Soc.* p. 837 (1947).

²J. Trotter, *Acta Crystallogr.* **16**, 698 (1963).

³J. W. Conant, H. H. Cady, R. R. Ryan, J. L. Yarnell, and J. M. Newsam, Los Alamos Technical Report LA-7756-MS, Los Alamos National Laboratory, 1979 (unpublished).

⁴H. H. Cady and A. C. Larson, *Acta Crystallogr., Sect. B: Struct. Crystallogr. Cryst. Chem.* **31**, 1864 (1975).

⁵J. J. Dick, *Appl. Phys. Lett.* **44**, 859 (1984).

⁶J. J. Dick, R. N. Mulford, W. J. Spencer, D. R. Pettit, E. Garcia, and D. C. Shaw, *J. Appl. Phys.* **70**, 3572 (1991).

⁷H. G. Gallagher, P. J. Halfpenny, J. C. Miller, and J. N. Sherwood, *Philos. Trans. R. Soc. London, Ser. A* **339**, 293 (1992).

⁸J. J. Dick, *J. Appl. Phys.* **81**, 601 (1997).

⁹Y. A. Gruzdkov and Y. M. Gupta, *J. Phys. Chem. A* **104**, 11169 (2000).

¹⁰C. S. Yoo, N. C. Holmes, P. C. Souers, C. J. Wu, F. H. Ree, and J. J. Dick, *J. Appl. Phys.* **88**, 70 (2000).

¹¹B. Olinger, P. M. Halleck, and H. H. Cady, *J. Chem. Phys.* **62**, 4480 (1975).

¹²B. Olinger and H. H. Cady, in *Sixth Symposium (International) on Detonation*, edited by D. J. Edwards (Office of Naval Research, Washington, D.C., 1976), p. 700.

¹³J. J. Dick and R. B. von Dreele, *Shock Compression of Condensed Matter* (AIP, Melville, 1997), p. 827.

¹⁴C. E. Morris, in *Sixth Symposium (International) on Detonation*, (Ref. 12), p. 396.

¹⁵J. M. Winey and Y. M. Gupta, *J. Appl. Phys.* **90**, 1669 (2001).

¹⁶J. J. Dick and J. P. Ritchie, *J. Appl. Phys.* **76**, 2726 (1994).

¹⁷D. C. Sorescu, B. M. Rice, and D. L. Thompson, *J. Phys. Chem. A* **103**, 989 (1999).

¹⁸D. C. Sorescu, B. M. Rice, and D. L. Thompson, *J. Phys. Chem. B* **103**, 6783 (1999).

¹⁹S. W. Bunte and H. Sun, *J. Phys. Chem. B* **104**, 2477 (2000).

²⁰A. Zaoui and W. Sekkal, *Solid State Commun.* **118**, 345 (2001).

²¹M. M. Kuklja and A. B. Kunz, *J. Appl. Phys.* **89**, 4962 (2001).

²²R. Dovesi, V. R. Saunders, C. Roetti, M. Causa, N. M. Harrison, R. Orlando, and E. Apra, *CRYSTAL95*,

- <http://www.chimifm.unito.it/teorica/crystal/>.
- ²³J. P. Perdew, K. Burke, and M. Ernzerhof, *Phys. Rev. Lett.* **77**, 3865 (1996).
- ²⁴M. Challacombe, E. Schwegler, C. Tymczak, C. K. Gan, K. Nemeth, A. M. N. Niklasson, H. Nymeyer, and G. Henkleman, MONDOSCF v1.0 α 7, A program suite for massively parallel, linear scaling SCF theory and *ab initio* molecular dynamics, 2001, URL <http://www.t12.lanl.gov/home/mchalla> [Los Alamos National Laboratory (LA-CC 01-2)], copyright University of California.
- ²⁵C. J. Tymczak and M. Challacombe (unpublished).
- ²⁶M. Challacombe, E. Schwegler, and J. Almlöf, *Computational Chemistry: Review of Current Trends* (World Scientific, Singapore, 1996), pp. 53-107.
- ²⁷M. Challacombe, E. Schwegler, and J. Almlöf, *J. Chem. Phys.* **104**, 4685 (1996).
- ²⁸M. Challacombe and E. Schwegler, *J. Chem. Phys.* **106**, 5526 (1997).
- ²⁹M. Challacombe, *J. Chem. Phys.* **113**, 10037 (2000).
- ³⁰C. K. Gan and M. Challacombe, *J. Chem. Phys.* **118**, 9128 (2003).
- ³¹J. Gump, L. Parker, and S. M. Peiris, in *13th APS Topical Conference on Shock Compression of Condensed Matter*, edited by Y. M. Gupta (American Physical Society, London, 2003).
- ³²T. D. Sewell (unpublished).
- ³³D. J. Pastine and R. R. Bernecker, *J. Appl. Phys.* **45**, 4458 (1974).
- ³⁴M. D. Murnaghan, *Finite Deformation of an Elastic Solid* (Dover, New York, 1951).
- ³⁵J. P. Poirier, *Introduction to the Physics of the Earth's Interior* (Cambridge, New York, 1991).
- ³⁶C. S. Yoo and H. Cynn, *J. Chem. Phys.* **111**, 10229 (1999).
- ³⁷R. Menikoff and T. D. Sewell, *High Press. Res.* **21**, 121 (2001).
- ³⁸T. D. Sewell, R. Menikoff, D. Bedrov, and G. D. Smith, *J. Chem. Phys.* **119**, 7417 (2003).
- ³⁹B. Olinger, B. Roof, and H. H. Cady, in *Proceedings of the International Symposium on High Dynamic Pressures* (CEA, Paris, 1978), p. 3.
- ⁴⁰F. L. Yarger and B. Olinger, *J. Chem. Phys.* **85**, 1534 (1986).